# Supplementary Materials

**Synthesis of ZSM-5 zeolites from biomass power plant ash for removal of ionic dyes from aqueous solution: Equilibrium isotherm, kinetic and thermodynamic analysis**

*Guangbing Liang [a], Yanhong Li [a]\*, Chun Yang [b], Xun Hu [c], Qingyin Li [c], Wenbo Zhao [a]*

[a] Faculty of Chemical Engineering, Kunming University of Science and Technology, Kunming, 650500, People's Republic of China
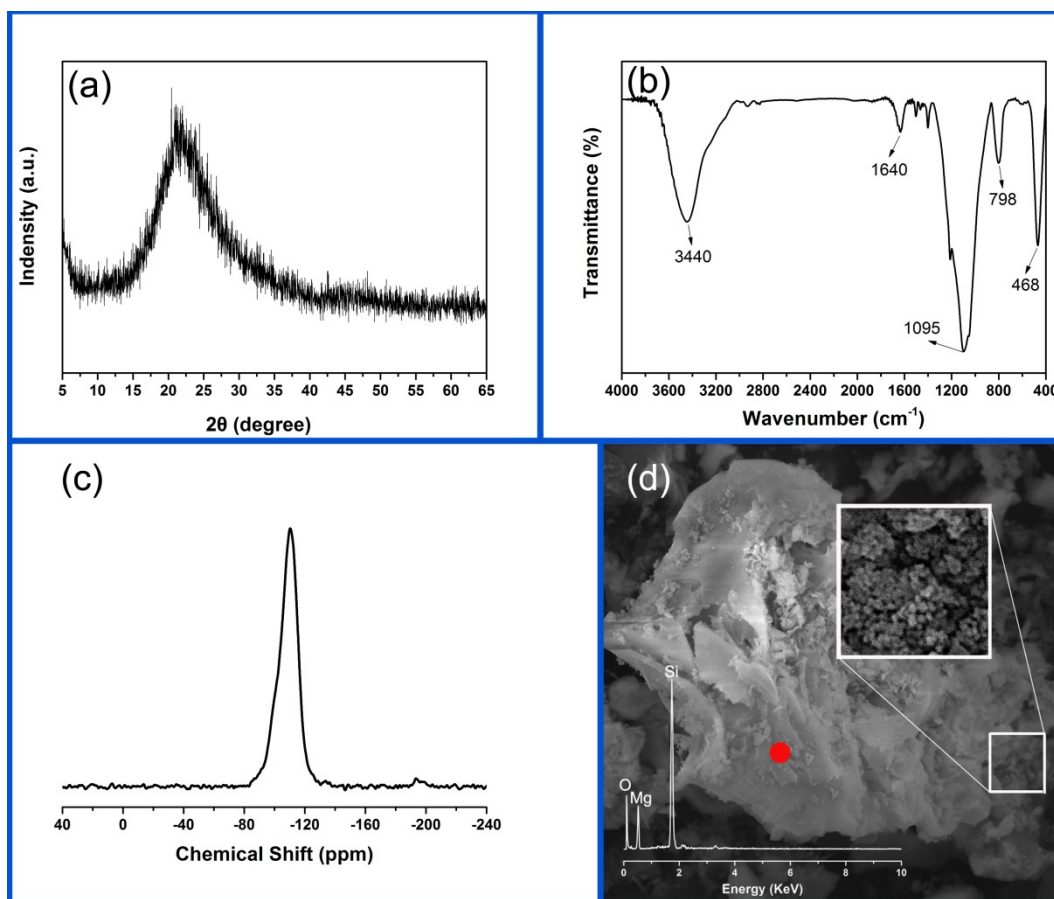
[b] College of Chemical Engineering and Environment, China University of Petroleum, Beijing, 102249, People's Republic of China

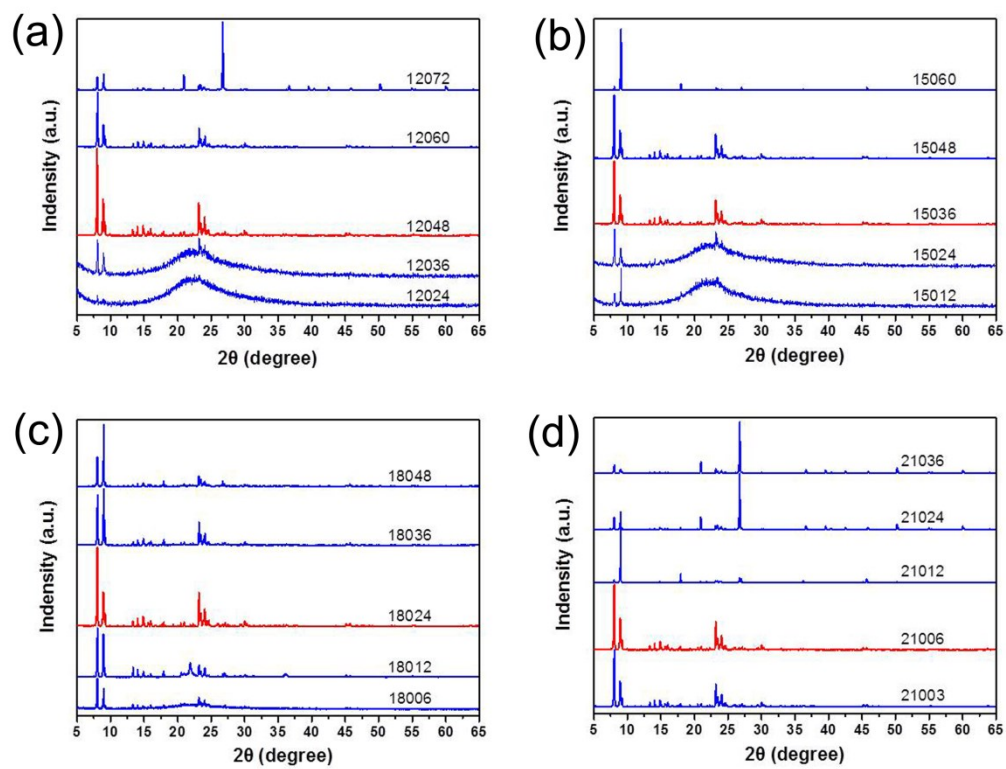[c] School of Material Science and Engineering, University of Jinan, Jinan, 250022, People's Republic of China

\* Corresponding Author: Yanhong Li, Tel: +86 15925236990

*E-mail address*: liyh_2004@163.com
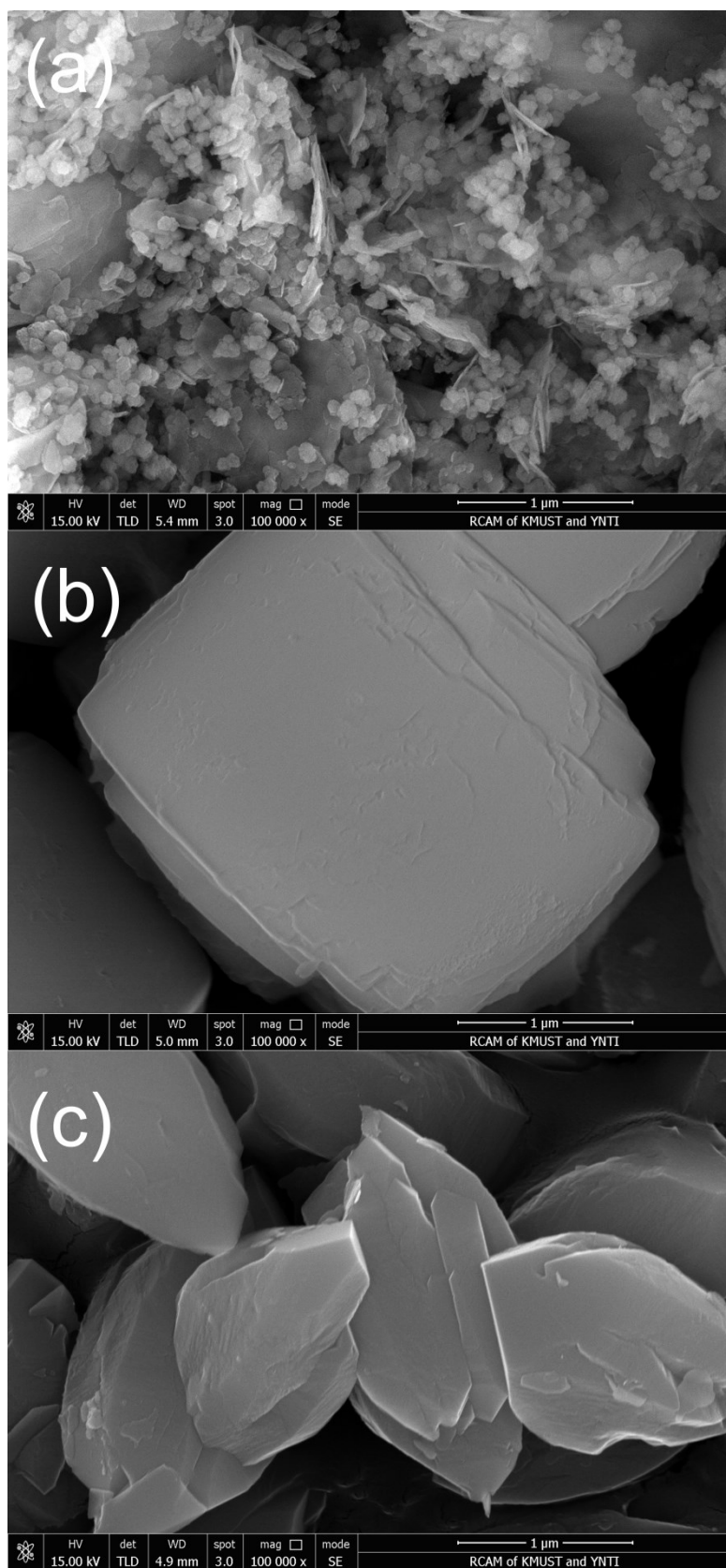
# 1. Figures



**Fig. S1** Characterization of the A-2: XRD (a), FTIR (b), $^{29}$Si MAS NMR (c), and SEM-EDX (d) analysis.

**Fig. S2** XRD analysis of synthesized zeolites under different conditions: 120 °C/24-72 h (a), 150 °C/12-60 h (b), 180 °C/6-48 h (c), and 210 °C/3-36 h (d).

**Fig. S3** Images of zeolite growth process at 120 $^oC$ for diverse times: 24 h (a), 48 h (b), and 72 h (c).
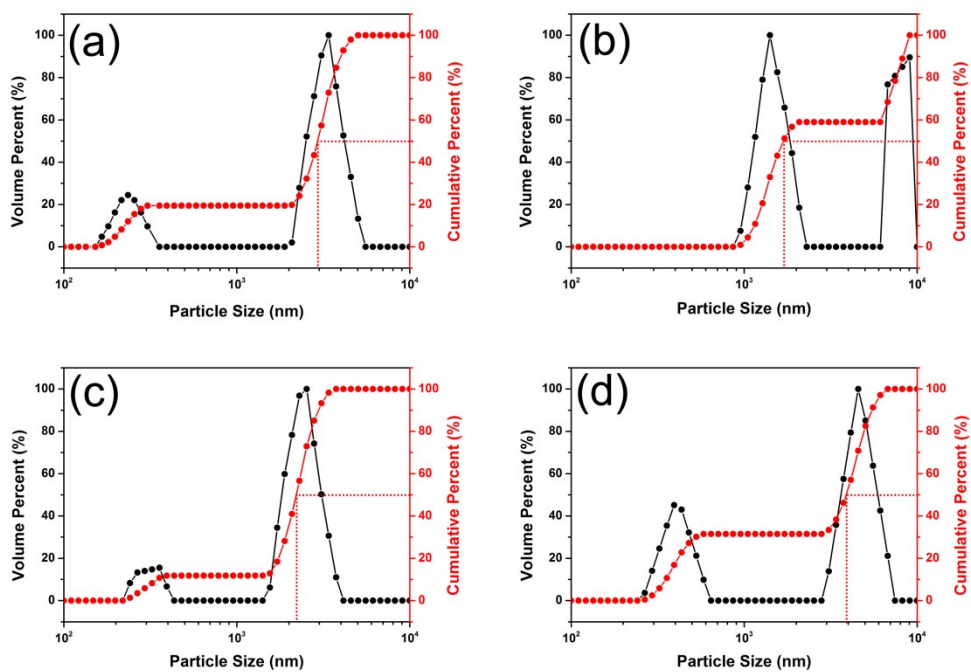
**Fig. S4** Particle size distribution of the ZSM-5 zeolites: Z-1 (a), Z-2 (b), Z-3 (c), and Z-4 (d).
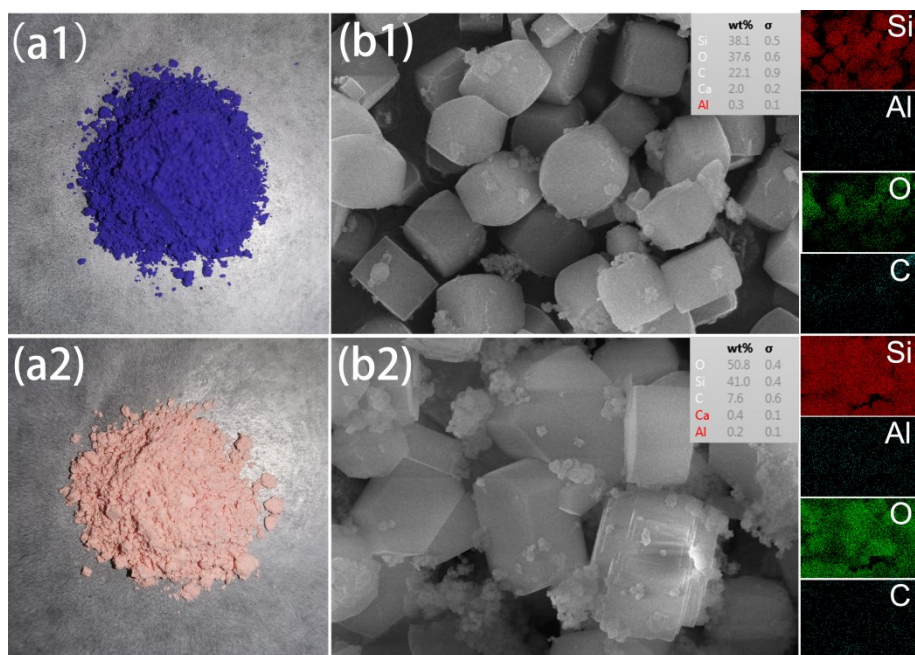
**Fig. S5** Digital photographs (a) and SEM images (b) coupled with EDX elemental mapping images of Si, Al, O and C after zeolite adsorbing MB (1) and CR (2) dyes.

The corresponding relation of temperature is as below:

25 °C — 298 K, 45 °C — 318 K and 65 °C — 338 K
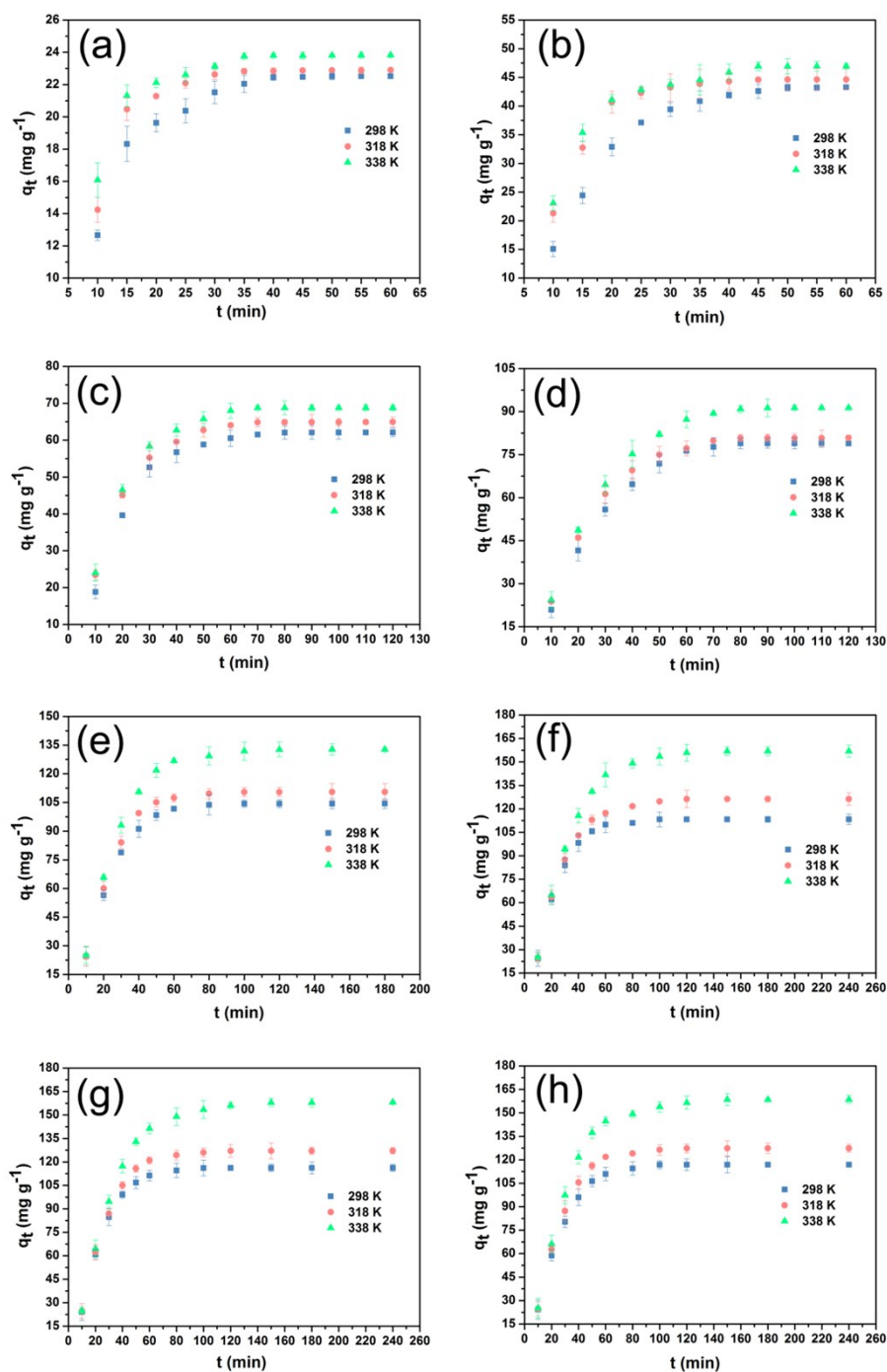


**Fig. S6** The variation of MB adsorption quantity with ZSM-5 zeolite adsorbent under diverse conditions: 25 mg/L (a), 50 mg/L (b), 75 mg/L (c), 100 mg/L (d), 200 mg/L (e), 300 mg/L (f), 400 mg/L (g) and 500 mg/L (h).
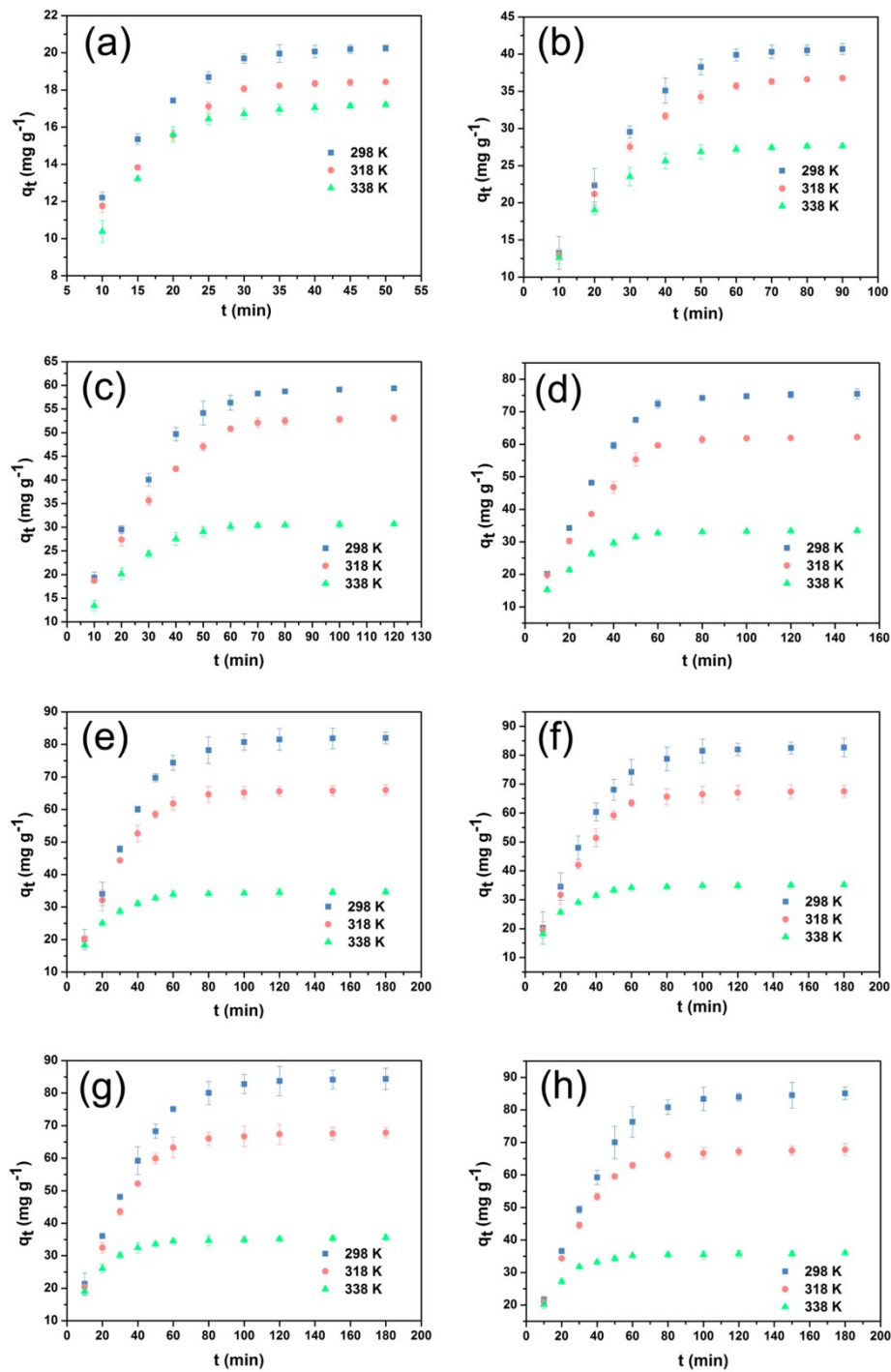
**Fig. S7** The variation of CR adsorption quantity with ZSM-5 zeolite adsorbent under diverse conditions: 25 mg/L (a), 50 mg/L (b), 75 mg/L (c), 100 mg/L (d), 200 mg/L (e), 300 mg/L (f), 400 mg/L (g) and 500 mg/L (h).
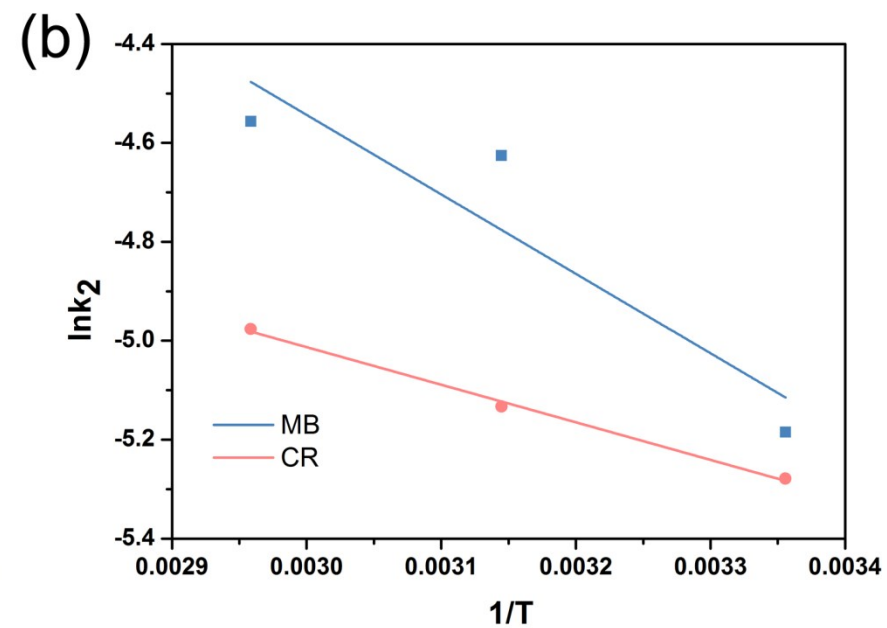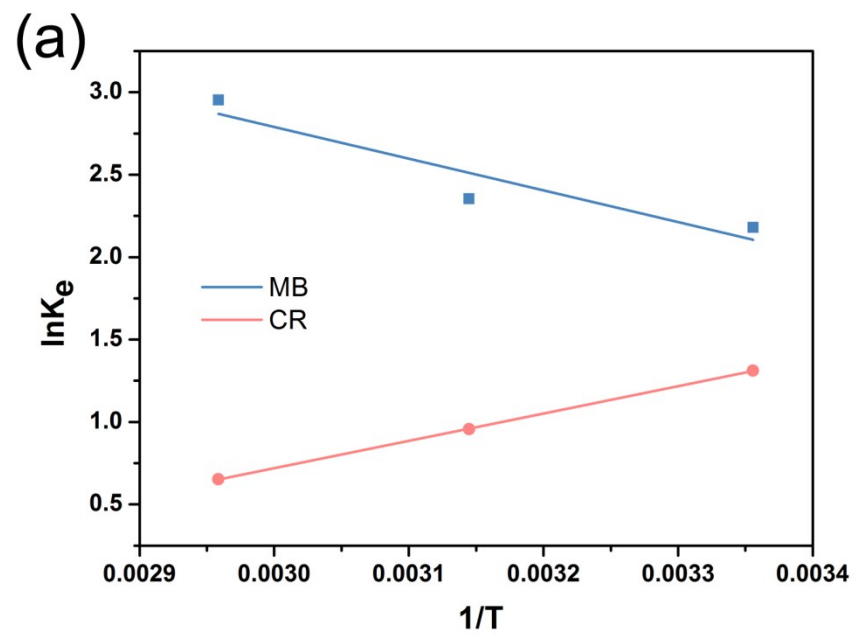
**Fig. S8** The fitting curves of the Van't Hoff (a) and the Arrhenius (b) plots at 25 mg/L initial dye concentration.

**2. Tables**

**Table S1** Chemical composition of A-1 and A-2 (Weight %).

| Sample | $SiO_2$ | CaO | $Al_2O_3$ | $Fe_2O_3$ | $K_2O$ | MgO | $Na_2O$ | $P_2O_5$ | $TiO_2$[*] |
|--------|---------|------|-----------|-----------|--------|------|---------|----------|-------------|
| A-1 | 44.41 | 23.84 | 10.80 | 3.63 | 3.99 | 3.76 | 1.27 | 2.02 | 1.05 |
| A-2 | 93.00 | 1.04 | 0.28 | 0.15 | 2.70 | 0.61 | 0.07 | 1.46 | - |

[*] Not detected in A-2.

**Table S2** The growth states of ZSM-5 zeolite under different hydrothermal conditions.

| t/h T/°C | 3 | 6 | 12 | 24 | 36 | 48 | 60 | 72 |
|---|---|---|---|---|---|---|---|---|
| 120 | × | × | × | + | + | ○ | - | - |
| 150 | × | × | + | + | ○ | - | - | × |
| 180 | × | + | + | ○ | - | - | × | × |
| 210 | + | ○ | - | - | - | × | × | × |

NOTE: × — Unnecessary to consider,

+ — Crystal growing,

○ — Crystal mature,

- — Crystal degradation or transition

**Table S3** Labeling of synthesized ZSM-5 zeolites.

| Sample labeling | Temperature, T/$^oC$ | Time, t/h |
| --- | --- | --- |
| Z-1 | 120 | 48 |
| Z-2 | 150 | 36 |
| Z-3 | 180 | 24 |
| Z-4 | 210 | 6 |

**Table S4** Textural properties of ZSM-5 zeolite samples.

| Sample | $S_{BET}$ (m²/g) | $S_{micro}$ (m²/g) | $S_{ext}$[a] (m²/g) | $V_{micro}$ (cm³/g) | $V_{meso}$ (cm³/g) | $D_{micro}$ (nm) | $D_{meso}$ (nm) | $d_{50}$[b] (μm) |
|---|---|---|---|---|---|---|---|---|
| Z-1 | 317.10 | 166.03 | 151.07 | 0.085 | 0.088 | 0.373 | 3.41 | 2.98 |
| Z-2 | 302.27 | 131.93 | 170.34 | 0.070 | 0.077 | 0.374 | 2.88 | 1.70 |
| Z-3 | 254.98 | 194.45 | 60.53 | 0.099 | 0.080 | 0.368 | 4.11 | 2.24 |
| Z-4 | 312.42 | 161.45 | 150.97 | 0.083 | 0.079 | 0.371 | 3.06 | 3.91 |

[a]Calculated from the subtraction between $S_{BET}$ and $S_{micro}$.

[b]Particle size accounted for 50% of total volume, illustration in Fig. S4.

**Table S5** Parameters of adsorption isothermal, kinetic and thermodynamic models.

| Dye | | MB | | | CR | | |
|---|---|---|---|---|---|---|---|
| Temperature, $^oC$ | | 25 | 45 | 65 | 25 | 45 | 65 |
| Removal efficiency, R% | | 89.84 | 91.32 | 95.04 | 78.76 | 72.24 | 65.76 |
| a. Isothermal model parameters | | | | | | | |
| Langmuir | $q_{max}$, mg/g | 120.00 | 130.46 | 160.24 | 87.49 | 70.31 | 35.88 |
| | $K_L$, L/mg | 0.0852 | 0.0921 | 0.1324 | 0.0972 | 0.0843 | 0.1124 |
| | $R^2$ | 0.9990 | 0.9961 | 0.9922 | 0.9589 | 0.9588 | 0.9959 |
| | $R_L$ | 0.3195 | 0.3028 | 0.2320 | 0.2915 | 0.3218 | 0.2625 |
| Freundlich | $K_F$, $(mg/g)/(L/mg)^{1/n}$ | 32.5171 | 34.7753 | 44.5263 | 30.3936 | 25.2063 | 16.9815 |
| | $1/n$ | 0.2295 | 0.2349 | 0.2341 | 0.1811 | 0.1733 | 0.1271 |
| | $R^2$ | 0.9370 | 0.9439 | 0.9393 | 0.8416 | 0.8413 | 0.9325 |
| Temkin | $b_T$, J/mol | 128.91 | 126.43 | 112.82 | 195.94 | 263.79 | 698.27 |
| | $K_T$, L/g | 1.7238 | 1.8124 | 2.6397 | 3.1361 | 3.1768 | 21.5983 |
| | $R^2$ | 0.9800 | 0.9853 | 0.9826 | 0.8833 | 0.8798 | 0.9486 |
| Sips | $q_{max}$, mg/g | 120.74 | 134.54 | 164.55 | 82.68 | 66.16 | 34.96 |
| | $K_S$, L/mg | 0.0838 | 0.0835 | 0.1193 | 0.0982 | 0.0820 | 0.1072 |
| | $\gamma$ | 0.9701 | 0.8753 | 0.8801 | 1.9433 | 1.9445 | 1.2658 |
| | $R^2$ | 0.9989 | 0.9970 | 0.9919 | 0.9966 | 0.9965 | 0.9988 |
| R−P | $K_{RP}$, L/g | 10.7033 | 13.9605 | 24.6669 | 5.9554 | 3.9353 | 3.4024 |
| | $\alpha$, $(L/mg)^{1/\beta}$ | 0.0962 | 0.1353 | 0.1956 | 0.0312 | 0.0233 | 0.0784 |
| | $\beta$ | 0.9864 | 0.9576 | 0.9552 | 1.1396 | 1.1552 | 1.0336 |
| | $R^2$ | 0.9990 | 0.9974 | 0.9932 | 0.9755 | 0.9804 | 0.9977 |
| b. Kinetic model parameters | | | | | | | |
| PFO | $q_{e,cal}$, mg/g | 29.76 | 43.84 | 18.80 | 30.47 | 25.03 | 49.91 |
| | $q_{e,exp}$, mg/g | 22.46 | 22.83 | 23.76 | 19.69 | 18.06 | 16.44 |
| | $k_1$, $min^{-1}$ | 0.1171 | 0.1736 | 0.1158 | 0.1339 | 0.1249 | 0.1988 |
| | $R^2$ | 0.9693 | 0.9607 | 0.9289 | 0.9878 | 0.9348 | 0.9155 |

| | | | | | | | |
|---|---|---|---|---|---|---|---|
| PSO | $q_{e,cal}$, mg/g | 25.69 | 24.88 | 25.65 | 24.08 | 21.78 | 20.11 |
| | $q_{e,exp}$, mg/g | 22.46 | 22.83 | 23.76 | 19.69 | 18.06 | 16.44 |
| | $k_2$, g/(g·min) | 0.0056 | 0.0098 | 0.0105 | 0.0051 | 0.0059 | 0.0069 |
| | $R^2$ | 0.9920 | 0.9928 | 0.9966 | 0.9934 | 0.9941 | 0.9899 |
| Intraparticle diffusion | $k_{p1}$, mg/(g·min$^{1/2}$) | 7.9498 | 8.7800 | 7.3589 | 3.2226 | 2.7777 | 3.3980 |
| | $|C_1|$, mg/g | 12.47 | 13.53 | 7.19 | 2.50 | 3.05 | 0.11 |
| | $k_{p2}$, mg/(g·min$^{1/2}$) | 1.7147 | 1.2024 | 1.1623 | 0.6152 | 0.3428 | 0.5572 |
| | $|C_2|$, mg/g | 11.85 | 15.91 | 16.84 | 16.32 | 16.19 | 13.66 |
| | $k_{p3}$, mg/(g·min$^{1/2}$) | 0.0454 | 0.0377 | 0.0294 | 0.2606 | 0.1074 | 0.2288 |
| | $|C_3|$, mg/g | 22.18 | 22.61 | 23.60 | 18.43 | 17.67 | 15.60 |
| c. Thermodynamic model parameters | | | | | | | |
| $\Delta G^0$, kJ/mol | | -5.40 | -6.22 | -8.30 | -3.25 | -2.53 | -1.83 |
| $\Delta H^0$, kJ/mol | | | 15.98 | | | -13.78 | |
| $\Delta S^0$, J/mol·K | | | 71.14 | | | -35.35 | |
| $E_a$, kJ/mol | | | 13.36 | | | 6.32 | |

## 3. Equations

Adsorption quantity:

$$q_t = \frac{V(C_0 - C_t)}{m}$$

(1)

Removal efficiency:

$$\%R = \frac{C_0 - C_t}{C_0} \times 100$$

(2)

Where $q_t$ is the dye adsorption quantity of adsorbent at t time, mg/g; $C_0$ and $C_t$ are the initial and t time concentrations of dye effluents, respectively, mg/L; V is the solution volume of dye effluents, L; and m is the mass of zeolite adsorbent, g.

Adsorption efficiency:

$$\%AE = \frac{q_{ex,exp}}{q_{e,exp}} \times 100$$

(3)

Where $q_{e,exp}$ is the experimental equilibrium adsorption quantity, mg/g; x is the cycle number, x=0, 1, 2, 3, 4 and 5. When x=0, $q_{ex,exp}$ is equal to $q_{e,exp}$.

Adsorption isothermal models:

Langmuir isotherm model is used to describe the maximum quantities of monolayer adsorption onto a homogeneous surface where the adsorption sites have equal affinity and energy without adsorbate-adsorbent interaction in the assumed conditions[1]. $R_L$ is a significant constant (dimensionless) related to adsorption behaviors of Langmuir isotherm.

$$q_e = q_{max} \frac{K_L C_e}{1 + K_L C_e}$$

(4)

$$R_L = \frac{1}{1 + K_L C_0}$$

(5)

Where $q_{max}$ is the maximum adsorption quantities, mg/g; $K_L$ is the Langmuir equilibrium

constant, L/mg. If $R_L>1$, the adsorption is unfavorable, and if $0<R_L<1$, the adsorption is favorable, while $R_L=0$ or 1, the adsorption is irreversible and linear, respectively.

Freundlich isotherm model is an empirical equation used to describe non-ideal multilayer adsorption in a heterogeneous system[2].

$$q_e = K_F C_e^{1/n} \tag{6}$$

Where $K_F$ is the Freundlich equilibrium constant, $(mg/g)/(L/mg)^{1/n}$; $1/n$ is the adsorption intensity. If $1/n>1$, the adsorption is unfavorable. On the contrary, If $0<1/n<1$, the adsorption is favorable, and it is irreversible when $1/n$ is equal to 0.

According to the trait of linear reduction of adsorption heat on the adsorbate-adsorbent molecule surfaces, Temkin isotherm model reflects that the bond energies between adsorbate and adsorbent, which is assumed to distribute uniformly[3].

$$q_e = \frac{RT}{b_T}\ln K_T + \frac{RT}{b_T}\ln C_e \tag{7}$$

Where $K_T$ is the Temkin equilibrium constant related to the bond energies between adsorbate and adsorbent, L/g; $b_T$ is the adsorption heat associated with adsorption rate in the initial stage, kJ/mol; R is the gas constant, 8.314 J/(mol·K).

Combined with Langmuir and Freundlich models, Sips isotherm model which is a three-parameter equation can be improved to express the heterogeneity of adsorption interaction[4]. As revealed, when the amount of adsorbent is large with low concentration of adsorbate, Sips model will trend to be the Langmuir model, otherwise the Freundlich model.

$$q_e = q_{max}\frac{(K_S C_e)^\gamma}{1+(K_S C_e)^\gamma} \tag{8}$$

Where $K_S$ is the Sips equilibrium constant, L/mg; $\gamma$ is the heterogeneity parameter. Herein,

the closer the $\gamma$ value is to 1, the more uniform the status is on the adsorbent surface.

Concerning on the absence of homogeneous adsorption in the Sips model, a three-parameter empirical equation of Redlich-Peterson isotherm model is put forward, which is suitable for either homogeneous or heterogeneous systems[5].

$$q_e = \frac{K_{RP}C_e}{1+\alpha C_e^{\beta}}$$ (9)

Where $K_{RP}$ is the Redlich-Peterson equilibrium constant, L/mg; $\alpha$ [(L/mg)$^{1/\beta}$] and $\beta$ ($0<\beta<1$) are the Redlich-Peterson isotherm parameters.

Adsorption kinetic models:

Generally speaking, PFO is assumed that one dye molecule would adhere onto one adsorption active site at the initial stage of adsorption process. Contrarily, PSO is assumed that one dye molecule would adhere onto two adsorption active sites on the whole adsorption process[6]. In particular, the diffusion rates are primarily determined by intraparticle diffusion and liquid film diffusion steps[7]. Thus, intraparticle diffusion model will make clear of the limiting step in adsorption stages. All the kinetic models were shown in a linear form as following:

$$\log(q_e - q_t) = \log q_e - \frac{k_1 t}{2.303}$$ (10)

$$\frac{t}{q_t} = \frac{t}{q_e} + \frac{1}{k_2 q_e^2}$$ (11)

$$q_t = k_{pi} t^{1/2} + C_i$$ (12)

Where $k_1$ is the adsorption rate constant of PFO model, min$^{-1}$; $k_2$ is the adsorption rate constant of PSO model, g/(mg·min); $k_p$ is the intraparticle diffusion constant, mg/(g·min$^{1/2}$); C is the correlation coefficient related to boundary layer thickness, mg/g; i is the order of

diffusion step (i=1, 2 and 3); t is the adsorption time, min.

Adsorption thermodynamic models:

To evaluate the thermodynamic properties during the zeolite adsorption process of MB and CR dyes, the parameters of $\Delta G^0$, $\Delta H^0$, $\Delta S^0$ and $E_a$ were put forward from the Van't Hoff and Arrhenius equations, which were given below:

$$K_d = \frac{q_e}{C_e} \tag{13}$$

$$\Delta G^0 = \Delta H^0 - T\Delta S^0 \tag{14}$$

$$\Delta G^0 = -RT \ln K_d \tag{15}$$

$$\ln K_d = -\frac{\Delta H^0}{RT} + \frac{\Delta S^0}{R} \tag{16}$$

$$\ln k_2 = \ln A - \frac{E_a}{RT} \tag{17}$$

Where $K_d$ is the adsorbate distribution coefficient, L/g; $\Delta H^0$ is the standard enthalpy, kJ/mol; $\Delta S^0$ is the standard entropy, J/(mol·K); $\Delta G^0$ is the standard Gibbs free energy, kJ/mol; $E_a$ is the activation energy, kJ/mol; A is the Arrhenius factor; T is the adsorption temperature, °C.

**Reference**

1. Oukil, S.; Bali, F.; Halliche, D., Adsorption and kinetic studies of methylene blue on modified HUSY zeolite and an amorphous mixture of γ-alumina and silica. *Separation Science and Technology* **2019**, 1-17.

2. Sabarish, R.; Unnikrishnan, G., Polyvinyl alcohol/carboxymethyl cellulose/ZSM-5 zeolite biocomposite membranes for dye adsorption applications. *Carbohydrate Polymers* **2018,** *199*, 129-140.

3. Nodehi, R.; Shayesteh, H.; Kelishami, A. R., Enhanced adsorption of congo red using

cationic surfactant functionalized zeolite particles. *Microchemical Journal* **2020,** *153*, 104281.

4.  Wang, Y.; Du, T.; Fang, X.; Jia, H.; Qiu, Z.; Song, Y., Synthesis of CO2-adsorbing ZSM-5 zeolite from rice husk ash via the colloidal pretreatment method. *Materials Chemistry and Physics* **2019,** *232*, 284-293.

5.  Hor, K. Y.; Chee, J. M. C.; Chong, M. N.; Jin, B.; Saint, C.; Poh, P. E.; Aryal, R., Evaluation of physicochemical methods in enhancing the adsorption performance of natural zeolite as low-cost adsorbent of methylene blue dye from wastewater. *J Clean Prod* **2016,** *118*, 197-209.

6.  Piri, F.; Mollahosseini, A.; Khadir, A.; Hosseini, M. M., Enhanced adsorption of dyes on microwave-assisted synthesized magnetic zeolite-hydroxyapatite nanocomposite. *Journal of Environmental Chemical Engineering* **2019,** *7* (5), 12.

7.  Wakkel, M.; Khiari, B.; Zagrouba, F., Textile wastewater treatment by agro-industrial waste: Equilibrium modelling, thermodynamics and mass transfer mechanisms of cationic dyes adsorption onto low-cost lignocellulosic adsorbent. *Journal of the Taiwan Institute of Chemical Engineers* **2019,** *96*, 439-452.